Selective Federated Learning for On-Road Services in Internet-of-Vehicles

Yuris Mulya Saputra, Diep N. Nguyen, Dinh Thai Hoang, and Eryk Dutkiewicz
School of Electrical and Data Engineering, University of Technology Sydney, Australia

***Abstract*—The Internet-of-Vehicles (IoV) can make driving safer and bring more services to smart vehicle (SV) users. Specifically, with IoV, the road service provider (RSP) can collaborate with SVs to provide high-accurate on-road information-based services by implementing federated learning (FL). Nonetheless, SVs' activities are very diverse in IoV networks, e.g., some SVs move frequently while other SVs are occasionally disconnected from the network. Consequently, obtaining information from all SVs for the learning process is costly and impractical. Furthermore, the quality-of-information (QoI) obtained by SVs also dramatically varies. That makes the learning process from all SVs simultaneously even worse when some SVs have low QoI. In this paper, we propose a novel selective FL approach for an IoV network to address these issues. Particularly, we first develop an SV selection method to determine a set of active SVs based on their location significance. In this case, we adopt a K-means algorithm to classify significant and insignificant areas where the SVs are located according to the areas' average annual daily flow of vehicles. From the set of SVs in the significant areas, we select the best SVs for the FL execution based on the SVs' QoI at each learning round. Through simulation results using a real-world on-road dataset, we observe that our proposed approach can converge to the FL results even with only 10% of active SVs in the network. Moreover, our results reveal that the RSP can optimize on-road services with faster convergence up to 63% compared with other baseline FL methods.**

Keywords- Federated learning, SV selection, vehicular networks, IoV, driving safety.

I. Introduction

The Internet-of-Vehicles (IoV) has emerged as one of the most promising solutions to enable efficient services for intelligent transportation systems, e.g., driving safety, traffic effectiveness, entertainment, and high economic efficiency. Based on Allied Market Research's outlook [1], the global market value of the IoV will increase significantly by 215% in 2024 due to the high demand of safe driving from smart vehicles (SVs), e.g., autonomous cars, driverless cars, and electric vehicles. Generally, the road service provider (RSP) can deploy on-road services to improve the driving safety for the SVs in the IoV. Specifically, the RSP can first collect data from active SVs, e.g., road conditions, location, and driving activities. Then, the RSP can extract the useful information based on the centralized learning process, aiming at improving on-road information accuracy [2]. To this end, the RSP can share the on-road information to other requesting SVs in various areas. In practice, the above approach has been widely implemented by some real-world on-road applications, e.g., the Placemeter (www.placemeter.com) and Google Maps (www.google.com/maps). However, sharing the actual data to the RSP in a centralized manner may lead to the privacy issue for the SV users, massive computation and storage cost for the RSP, as well as heavy network congestion in the IoV [3].

Recently, federated learning (FL) has been emerging as a cutting-edge distributed machine learning paradigm which can provide an effective learning collaboration model between the RSP and SVs without sharing any actual data in the network. In particular, the SVs can first train their local on-road data to produce local trained models. Then, the RSP only needs to collect the local models to update the global on-road information model, thereby improving the overall accuracy for the whole network with a low risk of information disclosure and minimum information exchange. For example, the authors in [4] and [5] study applications of FL-based learning models for diverse vehicular networks, e.g., communication delay evaluation for SVs and throughput improvement for autonomous driving. However, the previous works assume that all SVs can simultaneously send and receive the trained models to and from the RSP at every learning round, respectively. This requires excessive communications, especially in IoV networks with a huge number of SVs. In practice, some SVs may suffer from unreliable communication channels and even can be disconnected from the wireless connections due to the multiple handovers, Internet unavailability (e.g., the SVs visit uninhabited areas), or inactivity (e.g., the users turn off their SVs) at specific time. Additionally, SVs may have different quality-of-information (QoI) [6], e.g., some SVs may have very low QoI. These low-QoI SVs can induce a lower accuracy or unstable FL performance if their local models are aggregated together with other local models during the learning process [7]. As a result, the conventional FL models are costly and impractical to deploy in real-world IoV networks.

In this paper, we aim to develop a novel selective FL approach for the IoV network which can address the above limitations of conventional FL models. Specifically, the RSP can dynamically collaborate with the best active SVs based on the significance of their current locations and QoI for the FL process through the following three main steps at each learning round. First, the RSP can choose active SVs whose locations are within significant areas. These significant areas are determined based on the average annual daily flow (AADF), i.e., the average number of vehicles passing by all major roads on one day in a specific area [8]. As such, an area can be classified into a significant area if its AADF value is high. Second, the RSP can further select the best SVs based on their QoI (e.g., due to the RSP's incentive budget

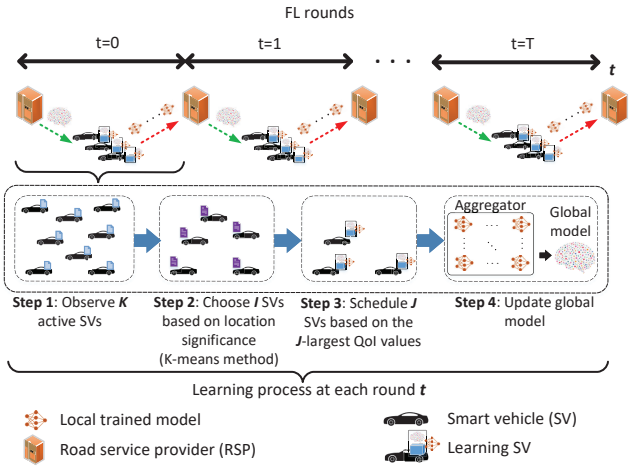

Fig. 1: The proposed selective FL model for the IoV network.

limitation for the SVs). Third, the best SVs can train the local on-road information models based on their local data obtained in this period and then send the trained models to the RSP for the global model update. Although there exist some selection methods which allow FL learners to join the FL process halfway, e.g., asynchronous FL [9], heterogeneity-based random selection [10], random scheduling (RS), round-robin (RR), and proportional fair (PF) methods [11], and local model processing time-based selection [12], all of them do not consider location significance and QoI-based selection which are the key factors for IoV networks. To the best of our knowledge, our selective FL approach is the first work accounting for both location significance and QoI of the participating SVs in the IoV network. Through simulation results, we show that our proposed approach can produce the convergence results of FL with accuracy level 85% using 10% of the active SVs in the network (which is proven to be converged theoretically). Furthermore, our proposed approach can outperform other baseline FL selection algorithms regarding the convergence speed of on-road information model accuracy by 62% and 63% for non independent and identically distributed (non-i.i.d), and i.i.d scenarios, respectively.

II. Selective FL Model for IoV Network

We illustrate the system model of the proposed selective FL for the IoV in Fig. 1. For each learning round, the RSP orchestrates the following steps:

1) The RSP observes K active SVs in the considered areas.
2) The RSP chooses I SVs from K SVs based on their location significance, i.e., within the significant areas (which are determined using K-means algorithm).
3) From I SVs, the RSP selects J best SVs which have the highest QoI values.
4) The selected J SVs train their own data to produce local trained models. These local models are then sent to the RSP to update the global model for the next round.

In this case, the RSP may select different set of best SVs at each round due to their various mobility activities. The above steps are repeated until the global on-road information model accuracy converges or after a pre-defined number of learning rounds is reached.

Let $\mathcal{K} = \{1, \ldots, k, \ldots, K\}$ denote the set of active SVs on the roads within the considered areas. Each SV-k can capture current on-road information using its available sensor devices (e.g., the camera, weather, and location sensors) periodically. Then, the SV can extract useful on-road information and store it in a log file at the SV's local storage. This information may contain the SV's visited location, date, time, light condition (e.g., dark or light), weather condition (e.g., windy, snowy, or rainy), and road surface condition (e.g., dry or wet). Using the log files, the RSP can select active SVs within its coverage (e.g., via road side units) to participate in the FL process. Specifically, the interested SV users can install an on-road service application developed by the RSP at their SVs' built-in Android devices, e.g., Live Traffic NSW [13]. To securely allow the RSP accessing basic information including the SVs' current location and QoI, the SV users can then enable the application's access permission. Note that the current location is only used to help the RSP select the best SVs for each learning round and can be anonymized using various location-based privacy methods [14] (e.g., used in Google Map and Uber). In this way, the RSP can observe useful information to choose the best SVs that work as the FL learners at each round, e.g., every hour, with the SVs' minimum privacy disclosure.

We denote $\mathcal{T} = \{0, 1, \ldots, t, \ldots, T\}$ to be the set of learning rounds. We define $\mathcal{I}(t) = \{1, \ldots, i, \ldots, I\}$, where $\mathcal{I}(t) \subset \mathcal{K}$, to be the set of selected SVs based on their location significance at round t. We also denote $\mathcal{J}(t) = \{1, \ldots, j, \ldots, J\}$, where $\mathcal{J}(t) \subset \mathcal{I}(t)$, to be the set of final best SVs based on their QoI at round t. We specify the collected data size, i.e., number of samples, at SV-j for t as $\sigma_j(t)$.

III. SV Selection Based on Location Significance and Quality of Information

In this section, we describe how the RSP can determine a set of SVs based on the location significance and QoI to execute the FL algorithm at each round t.

A. Location Significance-Based SV Selection

In this method, the RSP can observe the current location, i.e., latitude and longitude, of the active SVs through their global positioning system (GPS) information (stored at the on-road service application locally). From K SVs which enable the application, the RSP can choose I SVs, where $I \leq K$, whose locations are within the significant areas. These significant areas can be defined as the areas whose volume of the vehicle traffic is high through calculating their total AADFs for particular periods, e.g., big cities, central business districts, or tourist attractions. Suppose that $\mathcal{A} = \{1, \ldots, a, \ldots, A\}$ is the set of all considered areas. Then, the total AADF for each area-a can be expressed by $\Gamma_a = \sum_{y=1}^{y_{max}} \sum_{d=1}^{d_{max}} \frac{\gamma_a^{y,d}}{365}$ [8], where $\gamma_a^{y,d}$ indicates the vehicle volume in area-a for day-d of year-y. Furthermore, $y \in \{1, 2, \ldots, y_{max}\}$ and $d \in \{1, 2, \ldots, d_{max}\}$ represent the indices of considered year periods and days for a year (i.e., $d_{max} = 365$), respectively. The area with a

higher Γ_a value implies the area with higher significance. The reason is that many SV users tend to go to the centralized areas where better job market, preferable lifestyle, greater educational opportunities, and tourist attractions exist. As such, the vehicles in those crowded areas typically provide more useful and valuable on-road information, e.g., accident rate, due to their high volume of vehicle traffic [14].

Based on Γ_a, the RSP can classify the areas into insignificant and significant areas. In this case, we account for a binary categorization using K-means algorithm [15]. Suppose that the RSP has the road traffic information including area IDs, their major road locations, and their total AADFs $\Gamma_a, \forall a \in \mathcal{A}$. To obtain the sets of insignificant and significant areas (which are represented by '$-$' and '$+$', respectively), we need to find the total AADF centroids $\hat{\Gamma}^-$ and $\hat{\Gamma}^+$ that minimize the overall squared distance of each Γ_a and the centroids using the following optimization problem:

$$\min_{\{\boldsymbol{\pi}, \hat{\boldsymbol{\Gamma}}\}} \sum_{a \in \mathcal{A}} \pi_a^- (\Gamma_a - \hat{\Gamma}^-)^2 + \pi_d^+ (\Gamma_a - \hat{\Gamma}^+)^2, \tag{1}$$

$$\text{s.t.} \quad \pi_a^- + \pi_a^+ = 1, \forall a \in \mathcal{A}, \tag{2}$$

$$\pi_a^-, \pi_a^+ \in \{0, 1\}, \forall a \in \mathcal{A}, \tag{3}$$

where π_a^- and π_a^+ are binary variables specifying if the total AADF of area-a is closer to the centroids $\hat{\Gamma}^-$ and $\hat{\Gamma}^+$, respectively. The constraints in (2) describe that each area-a can be categorized into one group only.

To obtain the optimal sets of insignificant and significant areas, the centroids $\hat{\Gamma}^-$ and $\hat{\Gamma}^+$ are iteratively updated at each K-means iteration ς, i.e., $\hat{\Gamma}^-_{(\varsigma+1)} = \Big(\sum_{a \in \mathcal{A}} \pi^-_{a,(\varsigma)} \Gamma_a / \sum_{a \in \mathcal{A}} \pi^-_{a,(\varsigma)} \Big)$ and $\hat{\Gamma}^+_{(\varsigma+1)} = \Big(\sum_{a \in \mathcal{A}} \pi^+_{a,(\varsigma)} \Gamma_a / \sum_{a \in \mathcal{A}} \pi^+_{a,(\varsigma)} \Big)$, respectively, until $\hat{\Gamma}^-_{(\varsigma+1)} = \hat{\Gamma}^-_{(\varsigma)}$ and $\hat{\Gamma}^+_{(\varsigma+1)} = \hat{\Gamma}^+_{(\varsigma)}$. To this end, the RSP can decide the fixed optimal sets of insignificant areas, i.e., $\mathcal{A}^- \subset \mathcal{A}$, and significant areas, i.e., $\mathcal{A}^+ \subset \mathcal{A}$, based on the value '1' of π_a^- and π_a^+, $\forall a \in \mathcal{A}$, for all rounds. Then, the RSP can choose I SVs whose locations are in $\mathcal{A}^+$ at each t dynamically.

B. Quality of Information-Based SV Selection

Based on I SVs that are dynamically selected using the above SV selection, the RSP can further choose J SVs as the FL learners, where $J \leq I$, to efficiently implement the FL algorithm for each round t. Specifically, we introduce a QoI-based SV selection method to find J SVs which have the best information quality as described in the following. Consider that $\mathcal{G} = \{1, \ldots, g, \ldots, G\}$ and $\mathcal{H} = \{1, \ldots, h, \ldots, H\}$ to be the set of collected on-road information timespans, e.g., 7 days, and location IDs from the SVs in $\mathcal{I}(t)$, respectively. From each timespan-g and location-h, each SV-i can compute a spatio-temporal variability, i.e., the data size in location-h for timespan-g which can be denoted by $\sigma_i^{g,h}(t) \in [0, 1]$, from its total data size $\sigma_i(t)$ where $\sigma_i(t) = \sum_{g=1}^{G} \sum_{h=1}^{H} \sigma_i^{g,h}(t)$. This calculation is performed by the on-road service application.

To execute the FL at each round t, the RSP needs to determine the required spatio-temporal variability at timespan-g and location-h from SV-i, i.e., $\zeta_i^{g,h}(t)$. Since each SV-i, $i \in \mathcal{I}(t)$, likely has diverse mobile activities on the roads in various locations for different timespans, it may have dissimilar actual spatio-temporal variability for each timespan-g and location-h, which can be written as

$$d_i^{g,h}(t) = \begin{cases} \sigma_i^{g,h}(t), & \text{if } \sigma_i^{g,h}(t) \leq \zeta_i^{g,h}(t), \\ \zeta_i^{g,h}(t), & \text{otherwise.} \end{cases} \tag{4}$$

From $d_i^{g,h}(t)$ and $\zeta_i^{g,h}(t)$, we can define matrices of actual and required spatio-temporal variabilities for each SV-i as follows:

$$\mathbf{D}_i(t) = \begin{pmatrix} d_i^{1,1}(t) & d_i^{1,2}(t) & \cdots & d_i^{1,H}(t) \\ d_i^{2,1}(t) & d_i^{2,2}(t) & \cdots & d_i^{2,H}(t) \\ \vdots & \vdots & \ddots & \vdots \\ d_i^{G,1}(t) & d_i^{G,2}(t) & \cdots & d_i^{G,H}(t) \end{pmatrix} \tag{5}$$

and

$$\hat{\mathbf{D}}_i(t) = \begin{pmatrix} \zeta_i^{1,1}(t) & \zeta_i^{1,2}(t) & \cdots & \zeta_i^{1,H}(t) \\ \zeta_i^{2,1}(t) & \zeta_i^{2,2}(t) & \cdots & \zeta_i^{2,H}(t) \\ \vdots & \vdots & \ddots & \vdots \\ \zeta_i^{G,1}(t) & \zeta_i^{G,2}(t) & \cdots & \zeta_i^{G,H}(t) \end{pmatrix}. \tag{6}$$

Using (5) and (6), we can quantify the QoI metric as the normalized spatial length of a matrix in Frobenius norm, i.e.,

$$\eta_i(t) = 1 - \frac{\|\hat{\mathbf{D}}_i(t) - \mathbf{D}_i(t)\|_F}{\|\hat{\mathbf{D}}_i(t)\|_F}, \tag{7}$$

where $0 \leq \eta_i(t) \leq 1$ for each SV-i, $i \in \mathcal{I}(t)$. In particular, $\eta_i(t) = 0$ infers that no actual spatio-temporal variability is collected by the SV-i. Meanwhile, $\eta_i(t) = 1$ indicates that the required spatio-temporal variabilities for all timespans and location IDs of the SV-i fully hold. Using the QoI metric, the RSP can observe the dataset quality of SV-i, $\forall i \in \mathcal{I}(t)$, without requiring the SVs to share their actual datasets. Thus, the RSP can select J SVs to execute the FL algorithm according to their largest $\eta_i(t)$ values for each round t, i.e.,

$$\mathcal{J}(t) = \max_{[J]} \{\eta_1(t), \ldots, \eta_I(t)\}. \tag{8}$$

Equation (8) specifies that only J SVs will share their local models to update the global on-road information model accuracy at each round t of the FL process.

IV. FL WITH SV SELECTION ALGORITHM

A. FL with SV Selection Process

To obtain faster convergence when updating the global on-road information model accuracy, we execute the FL using the selected SVs in $\mathcal{J}(t)$ for each round t [7]. For the FL algorithm, we use deep neural networks (DNN) for a classification prediction model because the output layer of DNN produces discrete prediction values. Specifically, let $\mathbf{F}_j(t)$ and $\mathbf{L}_j(t)$ denote the training feature data (using features as columns) and ground-truth label data within $\sigma_j(t)$ of SV-j, $j \in \mathcal{J}(t)$, respectively, such that $\sigma(t) = \sum_{\mathcal{J}(t))} \sigma_j(t)$. Due to the use of multiple layers of the DNN, we have $\mathbf{F}_j^\ell(t)$ such that $\mathbf{F}_j^1(t) = \mathbf{F}_j(t)$, where ℓ is the training layer, $\ell \in [1, 2, \ldots, \ell_{max}]$. For each layer-$\ell$, we can compute the training output data as $\hat{\mathbf{L}}_j^\ell(t) = \rho_j^\ell\big(\mathbf{F}_i^\ell(t)\mathbf{X}(t)\big)$, where $\mathbf{X}(t)$ is the global on-road information model containing training weights. Additionally, $\rho_j^\ell(.)$ represents the activation

function of SV-j for nonlinear transformation. For layer-ℓ, $\ell \in [1, 2, \ldots, \ell_{max}-1]$, we use a *tanh* activation function, i.e., $\rho_j^{\ell}\big(\mathbf{F}_j^{\ell}(t)\mathbf{X}(t)\big) = \frac{e^{\mathbf{F}_j^{\ell}(t)\mathbf{X}(t)} - e^{-\mathbf{F}_j^{\ell}(t)\mathbf{X}(t)}}{e^{\mathbf{F}_j^{\ell}(t)\mathbf{X}(t)} + e^{-\mathbf{F}_j^{\ell}(t)\mathbf{X}(t)}}$. Furthermore, for the final layer, i.e., $\ell = \ell_{max}$, we adopt a *softmax* activation function (commonly used to interpret a probability distribution for classification model), i.e., $\rho_j^{\ell_{max}}\big(\mathbf{F}_j^{\ell}(t)\mathbf{X}(t)\big) = \frac{e^{\mathbf{F}_j^{\ell}(t)\mathbf{X}(t)}}{\sum e^{\mathbf{F}_j^{\ell}(t)\mathbf{X}(t)}}$.

We also use hidden layers ℓ, $1 < \ell < \ell_{max}$, to extract the meaningful features of the training input data. In this case, we can define that $\mathbf{F}_j^{\ell+1}(t) = \hat{\mathbf{L}}_j^{\ell}(t)$. At the final layer-$\ell_{max}$, we can produce the predicted label data $\hat{\mathbf{L}}_j^{\ell_{max}}(t)$ that are used to calculate the following SV-j's local loss function at each t

$$\psi_j\big(\mathbf{X}(t)\big) = \frac{1}{\sigma_j(t)} \sum_{r=1}^{\sigma_j(t)} \big(l_j^r(t) - \hat{l}_j^r(t)\big)^2, \tag{9}$$

where $l_j^r(t)$ and $\hat{l}_j^r(t)$ are the elements of ground truth label data $\mathbf{L}_j(t)$ and predicted label data $\hat{\mathbf{L}}_j^{\ell_{max}}(t)$ at row-r for round t, respectively. Using $\psi_j\big(\mathbf{X}(t)\big)$, we can compute the gradient of the local loss function at SV-j by $\nabla \mathbf{X}_j(t) = \frac{\partial \psi_j\left(\mathbf{X}(t)\right)}{\partial \mathbf{X}(t)}$. This $\nabla \mathbf{X}_j(t)$ can be used to update the local on-road information model $\mathbf{X}_j(t)$ which minimizes $\psi_j\big(\mathbf{X}(t)\big)$ for each SV-j by adopting the *Adam* optimizer as the adaptive learning rate. In particular, we can update the local update rules of the exponential moving average of the $\nabla \mathbf{X}_j(t)$, i.e., $m_j(t)$, and the squared $\nabla \mathbf{X}_j(t)$ to obtain the variance, i.e., $n_j(t)$, as the following formulas:

$$m_j^{(\nu+1)}(t) = \delta_{m_j}^{(\nu)}(t) m_j^{(\nu)}(t) + \big(1 - \delta_{m_j}^{(\nu)}(t)\big)\nabla \mathbf{X}_j(t), \tag{10}$$
$$n_j^{(\nu+1)}(t) = \delta_{n_j}^{(\nu)}(t) n_j^{(\nu)}(t) + \big(1 - \delta_{n_j}^{(\nu)}(t)\big)\big(\nabla \mathbf{X}_j(t)\big)^2,$$

where $\delta_{m_j}^{(\nu)}(t) \in [0, 1)$ and $\delta_{n_j}^{(\nu)}(t) \in [0, 1)$ specify the exponential decay steps of $m_j^{(\nu)}(t)$ and $n_j^{(\nu)}(t)$ at local epoch ν, respectively. Using the learning step ϕ_j, we can observe how frequently the $\mathbf{X}_j(t)$ is updated for the next local epoch $\nu+1$, which can be derived by $\phi_j^{(\nu+1)}(t) = \phi_j \frac{\sqrt{1-\delta_{n_j}^{(\nu+1)}(t)}}{1-\delta_{m_j}^{(\nu+1)}(t)}$.

Algorithm 1 The FL with SV Selection Algorithm

```
Set initial ν_th, T*, X(0), and t = 0
while t ≤ T* and Ψ(X(t)) does not converge do
    The RSP selects SVs in J(t) ⊂ I(t) ⊂ K using (8)
    for ∀j ∈ J(t) do
        Extract F_j(t) and L_j(t) from σ_j(t)
        Find L̂_j^{ℓ_max}(t) using F_j(t) and X(t)
        Compute ψ_j(X(t)) and send X_j^{(ν_th)}(t) to the RSP
    end for
    Update global model X(t+1) using X_j^{(ν_th)}(t) and σ_j, ∀j ∈ J(t)
    Evaluate global loss Ψ(X(t+1)) using ψ_j(X_j^{(ν_th)}(t)), ∀j ∈ J(t)
    t = t + 1
end while
Obtain the final global model X* and global loss Ψ*(X*)
```

Next, the $\mathbf{X}_j^{(\nu+1)}(t)$ for the next epoch $\nu+1$ can be updated by $\mathbf{X}_j^{(\nu)}(t) - \phi_j^{(\nu+1)}(t)\frac{m_j{}^{(\nu+1)}(t)}{\sqrt{n_j{}^{(\nu+1)}(t)}+\epsilon}$, where ϵ refers to a constant to avoid zero value of the $\sqrt{n_j{}^{(\nu+1)}(t)} + \epsilon$. This local iteration stops when a pre-defined local epoch threshold ν_{th} is reached, and thus we can produce the following variables $\phi_j^{(\nu_{th})}(t)$ and $\mathbf{X}_j^{(\nu_{th})}(t)$. Then, the SV-$j$ can send its $\mathbf{X}_j^{(\nu_{th})}(t)$ to the RSP for the global on-road information model update $\mathbf{X}(t+1)$ through aggregating all $\mathbf{X}_j^{(\nu_{th})}(t), \forall j \in \mathcal{J}(t)$, i.e.,

$$\mathbf{X}(t+1) = \frac{1}{\sigma(t)} \sum_{\mathcal{J}(t)} \sigma_j(t) \mathbf{X}_j^{(\nu_{th})}(t). \tag{11}$$

In this state, we can compute the global loss at $t+1$ as $\Psi(\mathbf{X}(t+1)) = \frac{1}{J}\sum_{\mathcal{J}(t)} \psi_j\Big(\mathbf{X}_j^{(\nu_{th})}(t)\Big)$. This global model update continues until the global loss converges or a pre-defined round threshold T^* is achieved. As a result, the final global model $\mathbf{X}^*$ and the final minimum global loss $\Psi^*(\mathbf{X}^*)$ can be obtained as summarized in Algorithm 1.

B. FL with SV Selection Convergence Analysis

We analyze the convergence of our proposed FL algorithm using the gap between the expected global loss after T^* rounds, i.e., $\mathbb{E}[\Psi(\mathbf{X}(T^*))]$ and the final global loss, i.e., $\Psi^*(\mathbf{X}^*)$. Suppose the probability that an SV will be selected for the FL process at any round is $\frac{J}{K}$. Then, we can show that the global loss gap is upper bounded by the expected squared L2-norm global model gap, i.e., $\mathbb{E}[\|\mathbf{X}(T^*) - \mathbf{X}^*\|_2^2]$, and lower bounded by zero as formally stated in the Theorem 1.

THEOREM 1. *The FL with the SV selection in Algorithm 1 will converge based on the global loss gap condition* $0 \leq \big[\mathbb{E}[\Psi(\mathbf{X}(T^*))] - \Psi^*(\mathbf{X}^*)\big] \leq \frac{\omega}{2}\mathbb{E}[\|\mathbf{X}(T^*) - \mathbf{X}^*\|_2^2]$, *where* ω *is a positive modulus from Lipschitz continuity.*

Proof. Due to limited space, we provide high-level ideas to prove Theorem 1 as follows. In particular, considering that the global loss function at any round $\Psi(\mathbf{X}(t))$ is ω-smooth, we can first show that $\big[\mathbb{E}[\Psi(\mathbf{X}(T^*))] - \Psi^*(\mathbf{X}^*)\big] \leq \frac{\omega}{2}\mathbb{E}[\|\mathbf{X}(T^*) - \mathbf{X}^*\|_2^2]$. Then, we can observe that $\lim_{T^*\to\infty}\big[\mathbb{E}[\Psi(\mathbf{X}(T^*))] - \Psi^*(\mathbf{X}^*)\big] = 0$ due to the decreasing learning rate $\lim_{t\to\infty}\phi_j^{(\nu_{th})}(t) = 0, \forall j \in \mathcal{J}(t)$. □

V. Performance Evaluation

A. Dataset Preparation

We evaluate the proposed selective FL approach using the actual two road traffic datasets in the United Kingdom (UK) between 2000 and 2016 [16]. For the first dataset, it contains 1.5M traffic accidents of all major roads in the UK with 34 features. From these features, we extract 7 important features including accident location with 416 location IDs, accident date, accident time, accident additional conditions, i.e., light, weather, and road surface conditions (as *training features*) and accident severity (as *training label*). For the second dataset, it includes 275K traffic AADFs from all major roads of 190 areas/local districts in the UK that will be used to find the set of significant areas. From the second dataset, we separate AADFs from all major roads based on the area IDs such that each area corresponds to a total AADF Γ_a.

B. Simulation Setup

To implement the proposed selective FL approach, we use *TensorFlow CPU 2.2*. We consider 100 SVs (i.e., $K = 100$)

Fig. 2: An illustration of significant (red) and insignificant (blue) areas in the UK from the dataset provided in [16].

to compare the performance of our proposed approach (considering location significance and QoI), i.e., PRO, with other baseline FL methods including random scheduling (RS) and round-robin scheduling (RR) [11]. For the RS and RR, the RSP chooses J SVs from all considered K SVs randomly and sequentially in a round-robin manner, respectively, without considering the SVs' location significance and QoI at each round. We also introduce a location-significance scheduling (LO) in which the RSP selects J SVs from I SVs randomly without accounting for the SVs' QoI at each round. From these SVs, we divide them into 3 categories, i.e., high-QoI SVs, medium-QoI SVs, and low-QoI SVs. Specifically, the data size and spatio-temporal variabilities will be generated in the following order: high-QoI SVs $>$ medium-QoI SVs $>$ low-QoI SVs. At each round, all SVs are randomly scattered in both significant and insignificant areas as illustrated in Fig. 2. We also consider different values of J, i.e., $1, 5,$ and 10 SVs, for each round to evaluate the efficiency of the PRO.

Next, we split the accident dataset into 0.8 training set and 0.2 testing set. Moreover, we consider non-i.i.d and i.i.d scenarios. For the non-i.i.d scenario, we first separate the training set randomly into 3 training subsets for high-QoI, medium-QoI, and low-QoI SVs. Then, we sort each training subset based on the training label. Each sorted training subset is distributed to the corresponding number of SVs based on their QoI. This scenario occurs when most of the learning SVs have only visited specific limited locations, e.g., the school bus or city public transport. Meanwhile, for the i.i.d scenario, we distribute accident training set randomly to the high-QoI, medium-QoI, and low-QoI SVs according to their QoI. This scenario takes place when most of the learning SVs have passed by many locations frequently, e.g., taxi or long-trip public transport. For the DNN, we use two hidden layers with 128 and 64 neurons per layer, and one final layer with 3 neurons (which correspond to 3 labels). In addition, we adopt the Adam optimizer with initial step size 0.01.

C. Simulation Results

1) Non-i.i.d scenario: We first evaluate the global model accuracy for the non-i.i.d scenario when the number of learning SVs, i.e., J, increases. In particular, the convergence speed gets faster when more learning SVs are selected at each round. As observed in Fig. 3(a), all FL methods suffer from the

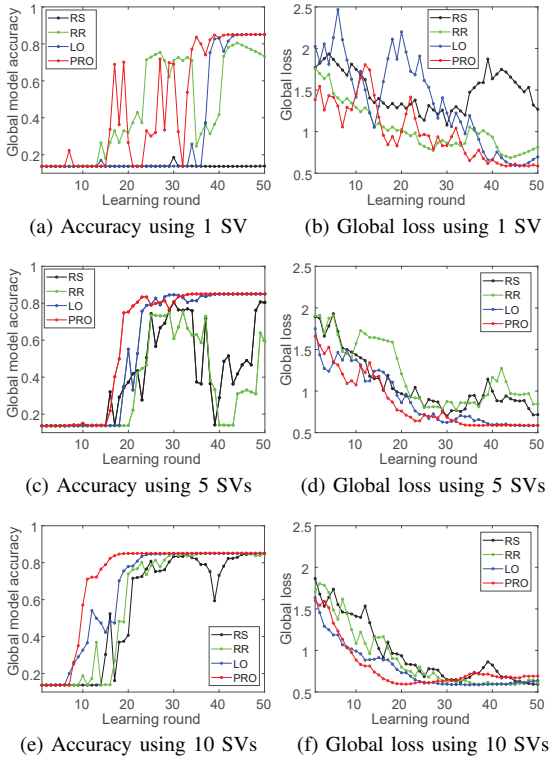

(a) Accuracy using 1 SV (b) Global loss using 1 SV

(c) Accuracy using 5 SVs (d) Global loss using 5 SVs

(e) Accuracy using 10 SVs (f) Global loss using 10 SVs

Fig. 3: The performance of proposed FL with SV selection using various learning SVs with non-i.i.d dataset.

fluctuated accuracy performance when the RSP only uses one learning SV (due to biased local dataset from each SV in K). This biased local dataset will produce inaccurate on-road information model and lead to the unstable FL performance [7]. Nonetheless, the PRO eventually can reach the convergence within 40 learning rounds with accuracy level 85%. In this case, the convergence speed of PRO outperforms that of LO up to 11.4% (or 5 rounds) because the selection of high-QoI SVs is guaranteed when we apply the PRO. Meanwhile, the RS and RR cannot even reach the convergence since they likely to select low-QoI SVs with very biased local datasets.

The accuracy performances for all FL methods improve when more learning SVs are selected by the RSP. As can be seen in Fig. 3(c) and Fig. 3(e), the PRO can speed up the accuracy convergence up to 13% (or 5 rounds) and 53% (or 20 rounds) when the RSP selects 5 and 10 learning SVs for each round, respectively. The reason is that the PRO can now train more high-QoI and medium-QoI SVs with less biased local datasets, and thus the unfairness among different SVs can be reduced. In this way, more accurate global on-road information model can be obtained faster. Furthermore, in terms of the accuracy convergence speed, the PRO can still outperform other baseline FL methods up to 17% (or 7 rounds) and 62% (or 29 rounds) when 5 and 10 learning SVs are utilized, respectively. These accuracy performances align with the global loss ones in Fig. 3(b), Fig. 3(d), and Fig. 3(f) where the PRO can reach the fastest minimum convergence compared with the baseline FL methods. To this end, the above results can provide insightful information for the RSP in practice to

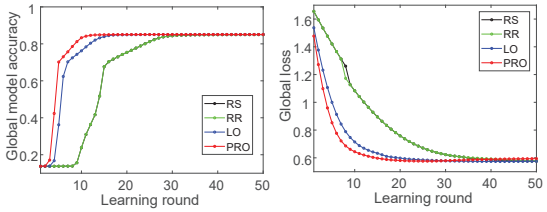

(a) Accuracy using 1 SV

(b) Global loss using 1 SV

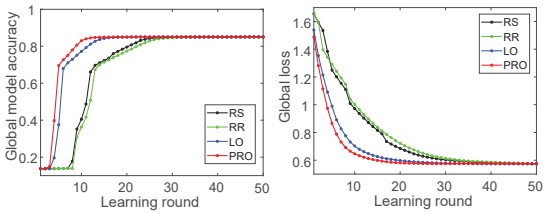

(c) Accuracy using 5 SVs

(d) Global loss using 5 SVs

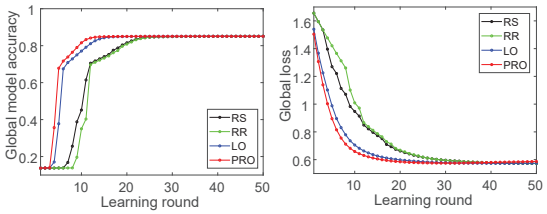

(e) Accuracy using 10 SVs

(f) Global loss using 10 SVs

Fig. 4: The performance of proposed FL with SV selection using various learning SVs with i.i.d dataset.

choose the best SV selection method for the FL process in terms of stability and flexibility in the IoV network.

2) i.i.d scenario: Next, we observe the global model accuracy for the i.i.d scenario for various number of learning SVs. When only one SV is used to execute the FL algorithm for each round as shown in Fig. 4(a), the PRO can converge 63% (or 22 rounds) faster than those of the RS and RR at accuracy level 85%. Additionally, the PRO can reach the convergence 35% (or 7 rounds) earlier than that of the LO at the same accuracy level. This is because the PRO only selects one SV with the highest QoI within the significant areas. Meanwhile, the RS and RR choose one learning SV from the total K SVs (due to no location significance and QoI-based SV selection method). As such, there exists high possibility that both methods choose only low-QoI SVs most of the learning rounds, which then slows down their convergence. For the LO, it only considers one learning SV in the significant areas without considering the QoI of SVs therein. Hence, the LO's accuracy convergence will be delayed slightly. Similar to the non-i.i.d scenario, the global loss in Fig. 4(b) aligns with the accuracy where the PRO and LO can reach the fastest convergence compared with those of the RS and RR.

The interesting point of accuracy performance can be observed when 5 and 10 learning SVs are considered in Fig. 4(c) and Fig. 4(e), respectively. Specifically, the RS, RR, and LO can improve the speed of accuracy convergence up to 23% (or 8 rounds) due to the existence of more accurate/meaningful local models from more learning SVs. Nonetheless, this trend does not apply for the PRO. The reason is that, with i.i.d local high-QoI dataset at each learning SV, the aggregation of all local models at the RSP will produce the same model accuracy compared with the case when one high-QoI SV is used. In this way, the additional datasets with the same high-QoI from other SVs will not further improve the convergence speed.

VI. Conclusion

In this paper, we have proposed a novel selective FL approach to address the limitations of conventional FL algorithm in the IoV network. In particular, we have introduced the location significance and QoI-based SV selection method which allows the RSP to select the best active SVs to implement FL algorithm for each learning round. Via the simulation results, we have shown that our proposed approach can produce high-accurate convergence results of FL without utilizing all SVs in the network simultaneously. Moreover, our proposed approach can outperform other baseline FL algorithms in terms of the convergence speed and provide insightful information to leverage more learning SVs for non-i.i.d scenario and one learning SV for i.i.d scenario to obtain the best FL performances.

References

[1] Internet of Vehicle Market Outlook: 2024, May 2018. Available Online: https://www.alliedmarketresearch.com/internet-of-vehicles-market. Last Accessed: Mar. 2021.

[2] W. Nie, *et al.*, "A quality-oriented data collection scheme in vehicular sensor networks," *IEEE Trans. Veh. Technol.*, vol. 67, no. 7, pp. 5570-5584, Jul. 2018.

[3] W. Y. B. Lim, *et al.*, "Federated learning in mobile edge networks: a comprehensive survey," *IEEE Commun. Surveys Tuts.*, vol. 22, no. 3, pp. 2031-2063, Apr. 2020.

[4] S. Samarakoon, *et al.*, "Federated learning for ultra-reliable low-latency V2V communications," in *IEEE GLOBECOM*, Dec. 2018, pp. 1-7.

[5] S. R. Pokhrel and J. Choi, "Improving TCP performance over WiFi for internet of vehicles: a federated learning approach," *IEEE Trans. Veh. Technol.*, vol. 69, no. 6, pp. 6798-6802, Jun. 2020.

[6] Z. Song, *et al.*, "QoI-aware multitask-oriented dynamic participant selection with budget constraints," *IEEE Trans. Veh. Technol.*, vol. 63, no. 9, pp. 4618-4632, Nov. 2014.

[7] M. Amiri, *et al.*, "Convergence of update aware device scheduling for federated learning at the wireless edge," arXiv:2001.10402 [cs.IT], May 2020.

[8] Road Traffic Estimates. Available Online: https://assets.publishing.service.gov.uk/government/uploads/system/uploads/attachment_data/file/524848/annual-methodology-note.pdf. Last Accessed: Mar. 2021.

[9] C. Xie, S. Koyejo, and I. Gupta, "Asynchronous federated optimization," arXiv:1903.03934 [cs.DC], Sept. 2019.

[10] T. Li, *et. al.*, "Federated optimization in heterogeneous networks," arXiv:1812.06127 [cs.LG], Apr. 2020.

[11] H. H. Yang, Z. Liu, T. Q. S. Quek, and H. V. Poor, "Scheduling policies for federated learning in wireless networks," *IEEE Trans. Commun.*, vol. 68, no. 1, pp. 317-333, Jan. 2020.

[12] W. Shi, S. Zhou, and Z. Niu, "Device scheduling with fast convergence for wireless federated learning," in *ICC 2020*, Jun. 2020, pp. 1-6.

[13] Live Traffic NSW. Available Online: https://www.livetraffic.com. Last Accessed: Mar. 2021.

[14] R. Hussain and S. Zeadally, "Autonomous cars: research results, issues, and future challenges," *IEEE Commun. Surveys Tuts.*, vol. 21, no. 2, pp. 1275-1313, Secondquarter 2019.

[15] P. S. Bradley, K. P. Bennett, and A. Demiriz, "Constrained K-means clustering," *Microsoft Research MSR-TR-2000-65*, May 2000.

[16] UK Traffic Accidents Between 2005 and 2014, Sept. 2017. Available Online: https://www.kaggle.com/daveianhickey/2000-16-traffic-flow-england-scotland-wales. Last Accessed: Mar. 2021.